

Studying the structural properties of polyalanine and polyglutamine peptides

Balázs Leitgeb · Ádám Kerényi · Ferenc Bogár ·
Gábor Paragi · Botond Penke · Gábor Rákely

Received: 15 June 2007 / Accepted: 8 August 2007 / Published online: 6 September 2007
© Springer-Verlag 2007

Abstract Poly-(Ala) and poly-(Gln) peptides have important biological effects, and can cause various human illnesses and neurodegenerative diseases. Conformational analysis of these homo-oligopeptides (HOPs) was carried out by simulated annealing in order to identify their structural properties regarding secondary structures and intramolecular H-bonding patterns. Poly-(Ala) and poly-(Gln) peptides composed of 7, 10, 14 or 20 amino acids were modelled in both charged and terminally blocked forms. In the case of conformers derived from simulated annealing calculations, the presence of various secondary structural elements (different types of β -turns, α -helix, 3_{10} -helix, poly-proline II helix, parallel and antiparallel β -strands) was investigated. Moreover, the intramolecular H-bonding patterns formed either between the backbone atoms for both HOPs or between the backbone and side-

chain atoms for the poly-(Gln) peptides were examined. Our results showed that different secondary structural elements (type I and type III β -turns, α -helix, 3_{10} -helix, antiparallel β -strand) could be observed in both poly-(Ala) and poly-(Gln) peptides and, according to their presence, characteristic H-bonding patterns formed mainly by $i \leftarrow i+3$ and $i \leftarrow i+4$ H-bonds could be found.

Keywords Homo-oligopeptides · Polyalanine · Polyglutamine · Secondary structure · Intramolecular H-bond

Introduction

Homo-oligopeptides (HOPs) are multimers of the same amino acid. The peptides poly-(Ala) and poly-(Gln) are probably the best known representatives of HOPs because they possess important biological effects, and can cause various human illnesses, playing a relevant role in the formation of several neurodegenerative diseases [1–3]. Therefore, detailed structural investigation of poly-(Ala) and poly-(Gln) peptides is important in order to identify their conformational properties, which can help in understanding the mechanisms underlying these human illnesses and neurodegenerative diseases.

Several experimental and theoretical studies have been performed so far to examine the structural features of poly-(Ala) and poly-(Gln) peptides as well as their derivatives. However, to determine the conformational properties of these molecules experimentally is a challenging task, because both of them are quite insoluble in water, and this insolubility leads to the aggregation of these HOPs. On the basis of previous experimental and theoretical studies, various structures have been proposed for both poly-(Ala) and poly-(Gln) peptides.

B. Leitgeb (✉) · Á. Kerényi · G. Rákely
Institute of Biophysics,
Biological Research Center of the Hungarian Academy of Sciences,
Temesvári krt. 62,
6726 Szeged, Hungary
e-mail: leitgeb@brc.hu

F. Bogár · G. Paragi · B. Penke
Supramolecular and Nanostructured Materials Research Group
of the Hungarian Academy of Sciences, University of Szeged,
Dóm tér 8,
6720 Szeged, Hungary

B. Penke
Department of Medical Chemistry, University of Szeged,
Dóm tér 8,
6720 Szeged, Hungary

G. Rákely
Department of Biotechnology, University of Szeged,
Temesvári krt. 62,
6726 Szeged, Hungary

Alanine is well-known to have a high propensity to form helical structures, especially α -helix. In accordance with this observation, α -helix was found to be the characteristic structure corresponding to the global minimum for Ace-(Ala)_n-NMe peptides, where n=8, 12, 16, or 19 [4–6]. Furthermore, based on the results of molecular dynamics simulations, predominantly α -helical conformation was observed in the case of poly-(Ala) peptides consisting of 15 or 20 residues [7–9]. Beside the α -helical structure, experimental investigations performed on Ala-based peptides suggested that β -helix could be formed in these molecules, especially at the N- and C-terminal ends [10–12]. Moreover, the coexistence of both α - and β -helical forms was proposed in the case of short Ala-based peptides [11]. The third helical structure observed for both poly-(Ala) and Ala-based peptides by experimental [13, 14] and theoretical [15, 16] investigations is the poly-proline II (PPII) helix. Molecular dynamics calculations pointed out the coexistence of α - and PPII helical conformations for the Ace-(Ala)₂₁-NMe peptide [17]. However, not only helical structures have been found for poly-(Ala) peptides. Theoretical studies revealed that for the poly-(Ala) composed of 12 amino acids, the stable state was α -helix in vacuum, while this helical conformation was destabilised in aqueous medium, in which the β -structure became the stable state [18].

Similarly to poly-(Ala) peptides, various structures have also been suggested for poly-(Gln) molecules [19]. Based on the results of experimental and theoretical investigations, a predominantly random coil or unordered conformation was observed for poly-(Gln) and Gln-based peptides of different lengths [20–22]. In addition, in the case of a peptide composed of 15 Gln residues, a β -structure made of antiparallel β -strands was proposed [23], in which the monomers formed hairpins stabilized by H-bonds. Similar observations were made for the poly-(Gln)₂₂ peptide and Gln-based molecules possessing histidine amino acids [24]. Finally, a helical conformation with 20 amino acids per turn, which was called β -helix, was also suggested in the case of poly-(Gln) peptides consisting of more than 35–40 residues [25, 26].

As mentioned above, poly-(Ala) and poly-(Gln) peptides are known to cause a variety of human illnesses and neurodegenerative diseases. Therefore, the aims of our study were to perform conformational analysis and detailed structural investigation focusing on the secondary structural elements and the intramolecular H-bonding patterns of the charged and blocked forms of poly-(Ala) and poly-(Gln) peptides consisting of 7, 10, 14 or 20 residues.

Methods

For the conformational analysis of poly-(Ala)_n and poly-(Gln)_n peptides of different lengths ($n=7, 10, 14$ and 20),

simulated annealing (SA) calculations were carried out using AMBER 9 software [27]. In the case of SA simulations, the AMBER 99 force field [28] and the Generalized Born (GB) solvent model (i.e. the Hawkins, Cramer, Truhlar pairwise GB model) [29, 30] were used, and no cut-off was applied for the non-bonding interactions.

The SA protocol applied to explore the conformational space of HOPs was the following. Each SA procedure was started from a structure characterised by an extended peptide backbone, which was optimised by an energy minimisation. Following the initial geometry optimisation, the structures were first heated to 1,000 K during 1,000 fs, equilibrated at 1,000 K for 4,000 fs, and finally the temperature was decreased to 50 K for 10,000 fs using a multistep (near-exponential) cooling protocol composed of three consecutive linear stages. The SA cycle consisting of heating, equilibration and cooling was repeated 1,000 times, resulting in 1,000 conformers for each HOP. For the structures supplied by the SA protocol, a final energy minimisation was performed using the conjugated gradient method with a convergence criterion of 0.005 kcal mol^{−1} Å^{−1} applied to the gradient.

The poly-(Ala)_n and poly-(Gln)_n peptides were modelled in two different forms: (1) molecules with charged N-terminal amino and C-terminal carboxyl groups, (2) molecules with the N- and C-terminal ends blocked by acetyl (Ac) and N-methyl amide (NMe) groups, respectively.

Results and discussion

Secondary structures

For the conformers obtained by SA calculations, the presence of the following secondary structural elements was investigated: different types of β -turns, α -helix, β -helix, PPII helix, parallel and antiparallel β -strands. To determine these secondary structures, the characteristic ranges of Φ and Ψ torsion angles were applied for different turns as well as helices and strands (see Table 1). The occurrence of various β -turns was examined for each tetrapeptide unit of the sequences. In the case of helices and strands, three consecutive amino acids satisfying certain Φ and Ψ torsion angle criteria were considered to be the minimum secondary structural element. However, periodic structures evolved in longer segments (i.e. tetra- and pentapeptide units, and so on) were also investigated along the entire sequence of peptides.

For the poly-(Ala)_n and poly-(Gln)_n peptides, mainly two types of β -turns (type I and type III) were observed, which appeared in each tetrapeptide segment along the entire sequence of molecules. Table 2 shows the minimum (β I_{min}, β III_{min}), maximum (β I_{max}, β III_{max}) and average (β I_{ave}, β III_{ave}) populations as well as the total numbers of

Table 1 Characteristic ranges of the Φ and Ψ torsion angles applied to determine different turns, helices and strands. *PPII* Poly-proline II

Ranges of Φ and Ψ torsion angles				
β -turns	Φ_{i+1}	Ψ_{i+1}	Φ_{i+2}	Ψ_{i+2}
Type I β -turn	$-60^\circ \pm 30^\circ$	$-30^\circ \pm 30^\circ$	$-90^\circ \pm 30^\circ$	$0^\circ \pm 30^\circ$
Type II β -turn	$-60^\circ \pm 30^\circ$	$120^\circ \pm 30^\circ$	$80^\circ \pm 30^\circ$	$0^\circ \pm 30^\circ$
Type III β -turn	$-60^\circ \pm 30^\circ$	$-30^\circ \pm 30^\circ$	$-60^\circ \pm 30^\circ$	$-30^\circ \pm 30^\circ$
Type V β -turn	$-80^\circ \pm 30^\circ$	$80^\circ \pm 30^\circ$	$80^\circ \pm 30^\circ$	$-80^\circ \pm 30^\circ$
Periodic secondary structures				
	Φ_i	Ψ_i		
α -helix	$-60^\circ \pm 30^\circ$	$-50^\circ \pm 30^\circ$		
β_10 -helix	$-60^\circ \pm 30^\circ$	$-30^\circ \pm 30^\circ$		
PPII helix	$-75^\circ \pm 30^\circ$	$145^\circ \pm 30^\circ$		
Parallel β -strand	$-120^\circ \pm 30^\circ$	$120^\circ \pm 30^\circ$		
Antiparallel β -strand	$-140^\circ \pm 30^\circ$	$140^\circ \pm 30^\circ$		

β -turns (β I_{sum} , β III_{sum}) found in all the tetrapeptide units for type I and type III β -turns, respectively. The values of β I_{sum} and β III_{sum} indicated that, in the case of HOPs, the populations of the type III β -turn were larger compared to those of the type I β -turn. Furthermore, these results also revealed that the poly-(Ala)_n peptides showed greater propensity to form β -turns than the poly-(Gln)_n peptides. Additionally, the above-mentioned cumulative values pointed out that, for the terminally blocked molecules, more β -turns appeared in the majority of cases than with charged molecules. These differences can be explained by comparing the β -turn populations observed at both the N- and the C-terminal tetrapeptide units for the charged and blocked forms of HOPs. In the case of charged molecules, lower

proportions of β -turns were found for the N- and C-terminal tetrapeptide segments, but in the blocked molecules the populations of β -turns evolving in the units mentioned above did not differ substantially from those occurring in any other tetrapeptide segment of the peptides. The values of β I_{min} and β III_{min} also demonstrated these differences between the zwitterionic and terminally blocked forms of HOPs, and each of these populations was located at either the N-terminal or the C-terminal tetrapeptide units of the charged molecules.

In the case of HOPs, in addition to structures characterized by one β -turn, several conformers were observed, in which two or more β -turns appeared at the same time either consecutively or in separated tetrapeptide units. As indicat-

Table 2 Minimum (β I_{min} , β III_{min}), maximum (β I_{max} , β III_{max}), and average (β I_{ave} , β III_{ave}) populations (in number) and the total numbers of β -turns (β I_{sum} , β III_{sum}) found in the tetrapeptide units for type I and type III β -turns. *HOP* Homo-oligopeptide

HOP	Populations of β I turns				Populations of β III turns			
	β I_{min}	β I_{max}	β I_{ave}	β I_{sum}	β III_{min}	β III_{max}	β III_{ave}	β III_{sum}
$\text{H}_3\text{N}^+-(\text{Ala})_7-\text{COO}^-$	44	128	87	346	71	167	122	487
Ace-(Ala) ₇ -NMe	72	95	84	337	155	196	179	714
$\text{H}_3\text{N}^+-(\text{Gln})_7-\text{COO}^-$	21	56	39	157	18	71	48	192
Ace-(Gln) ₇ -NMe	43	70	58	231	74	94	86	343
$\text{H}_3\text{N}^+-(\text{Ala})_{10}-\text{COO}^-$	40	104	81	569	60	166	125	877
Ace-(Ala) ₁₀ -NMe	81	99	90	629	133	176	154	1,075
$\text{H}_3\text{N}^+-(\text{Gln})_{10}-\text{COO}^-$	22	52	38	267	22	67	51	354
Ace-(Gln) ₁₀ -NMe	47	59	51	358	66	80	73	512
$\text{H}_3\text{N}^+-(\text{Ala})_{14}-\text{COO}^-$	50	99	80	877	62	162	136	1,501
Ace-(Ala) ₁₄ -NMe	67	98	78	862	126	152	141	1,552
$\text{H}_3\text{N}^+-(\text{Gln})_{14}-\text{COO}^-$	27	56	40	442	29	75	55	600
Ace-(Gln) ₁₄ -NMe	32	51	42	462	50	71	59	649
$\text{H}_3\text{N}^+-(\text{Ala})_{20}-\text{COO}^-$	37	104	73	1,238	53	154	127	2,160
Ace-(Ala) ₂₀ -NMe	65	93	75	1,282	103	156	132	2,248
$\text{H}_3\text{N}^+-(\text{Gln})_{20}-\text{COO}^-$	14	46	34	579	17	71	48	816
Ace-(Gln) ₂₀ -NMe	28	47	37	625	33	65	51	865

ed by the results shown in Table 3, the cumulative numbers (Sum) of multiple appearance of type III β turns were larger for both the poly-(Ala)_n and the poly-(Gln)_n peptides than those of type I β -turns. Additionally, differences were observed between the maximum numbers of type I and type III β -turns occurring simultaneously in the conformers. In the case of type I β -turns, the maximum numbers of turn structures were smaller compared to those of type III β -turns. For example, in the H₃N⁺-(Ala)₂₀-COO⁻ peptide, 5 and 10 were the maximum numbers of type I and type III β -turns, respectively. As mentioned previously, poly-(Ala)_n peptides showed a greater propensity to form β -turns than poly-(Gln)_n peptides and, in accordance with this observation, the proportions of multiple turn structures were larger for the former than for the latter HOPs. Figure 1 shows one representative of these multiple turn structures for the

H₃N⁺-(Ala)₇-COO⁻ peptide, in which two type III β -turns appear at the same time at the N-terminal (Ala¹-Ala²-Ala³-Ala⁴) and the C-terminal (Ala⁴-Ala⁵-Ala⁶-Ala⁷) tetrapeptide units.

The examination of periodic secondary structures (α -helix, 3₁₀-helix, PPII helix, parallel and antiparallel β -strands) disclosed the appearance of mainly α - and 3₁₀-helical segments as well as antiparallel β -strand-like segments for the poly-(Ala)_n and poly-(Gln)_n peptides. Table 4 shows the relative populations compared to the total number of different tripeptide motifs (M_T) for the three above-mentioned conventional periodic secondary structures (α -helix: $\alpha\alpha\alpha$, 3₁₀-helix: 3₁₀3₁₀3₁₀, β -strand: $\beta\beta\beta$) evolved in the tripeptide units along the entire sequence of molecules. In the case of helices and β -strand, average ratios (M_{Ave}) were calculated for charged poly-(Ala)_n,

Table 3 Number of conformers containing two or more β -turns at the same time either consecutively or in separated tetrapeptide units for type I and type III β -turns

Number of turns	β I	β III	β I	β III	β I	β III	β I	β III
		H ₃ N ⁺ -(Ala) ₇ -COO ⁻		Ace-(Ala) ₇ -NMe		H ₃ N ⁺ -(Gln) ₇ -COO ⁻		Ace-(Gln) ₇ -NMe
2	29	40	23	68	15	25	21	45
3	1	35		49	2	6		15
4		12		42				5
Sum ^a	30	87	23	159	17	31	21	65
		H ₃ N ⁺ -(Ala) ₁₀ -COO ⁻		Ace-(Ala) ₁₀ -NMe		H ₃ N ⁺ -(Gln) ₁₀ -COO ⁻		Ace-(Gln) ₁₀ -NMe
2	88	83	109	126	39	65	50	74
3	9	61	11	64	3	14	10	33
4		33		46		2	1	12
5		9		13		1		1
6		3		9				0
7		1						1
Sum	97	190	120	258	42	79	61	121
		H ₃ N ⁺ -(Ala) ₁₄ -COO ⁻		Ace-(Ala) ₁₄ -NMe		H ₃ N ⁺ -(Gln) ₁₄ -COO ⁻		Ace-(Gln) ₁₄ -NMe
2	178	164	174	183	73	91	75	101
3	28	79	25	92	14	27	18	38
4	6	71	4	51	2	14		13
5	1	27	1	37		5		4
6		16		20		1		2
7		10		8		1		1
8		3		2		0		
9		2		3		1		
Sum	213	372	204	396	89	140	93	159
		H ₃ N ⁺ -(Ala) ₂₀ -COO ⁻		Ace-(Ala) ₂₀ -NMe		H ₃ N ⁺ -(Gln) ₂₀ -COO ⁻		Ace-(Gln) ₂₀ -NMe
2	244	195	274	210	89	111	115	133
3	87	112	83	128	30	52	23	46
4	21	93	22	83	2	15	7	23
5	2	58	2	53	1	12		13
6		34		40		3		2
7		19		21		2		1
8		8		14				
9		8		5				
10		1		1				
Sum	354	528	381	555	122	195	145	218

^a Sum = the cumulative numbers of multiple appearance of type I or type III β -turns

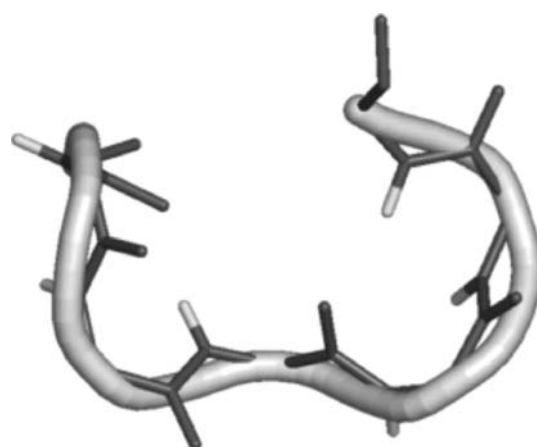


Fig. 1 One representative of the multiple turn structures for the H_3N^+ -(Ala)₇-COO[−] peptide, in which two type III β -turns appear at the same time at the N-terminal (Ala¹-Ala²-Ala³-Ala⁴) and the C-terminal (Ala⁴-Ala⁵-Ala⁶-Ala⁷) tetrapeptide units. Only the peptide backbone is represented by both sticks and ribbon

blocked poly-(Ala)_n, charged poly-(Gln)_n and blocked poly-(Gln)_n peptides. From the values of relative populations and $M_{\text{Ave}}-\text{s}$, it can be seen that for the poly-(Ala)_n peptides, predominantly $\alpha\alpha\alpha$ and $3_{10}3_{10}3_{10}$ structures were found, while populations of the $\beta\beta\beta$ motif were lower compared to the above-mentioned values. However, for the poly-(Gln)_n peptides, mainly $3_{10}3_{10}3_{10}$ and $\beta\beta\beta$ structures were

observed, and the $\alpha\alpha\alpha$ motif appeared with the lowest frequency [with the exception of the Ace-(Gln)₇-NMe and Ace-(Gln)₁₀-NMe molecules, where the relationship between the populations of $\beta\beta\beta$ and $\alpha\alpha\alpha$ structures was the opposite in comparison with the other peptides]. Comparing the relative populations of three investigated motifs for the zwitterionic and terminally blocked forms of HOPs, it can be seen that, in the case of blocked peptides consisting of 7 or 10 amino acids, the proportions of $\alpha\alpha\alpha$ and $3_{10}3_{10}3_{10}$ structures were larger, while the populations of $\beta\beta\beta$ motifs were lower compared to those of charged molecules with the same length. Interestingly, these differences between the two forms depending on the ionisation state were smaller in the case of HOPs composed of 14 or 20 residues. These results revealed that differences between the relative populations of $\alpha\alpha\alpha$, $3_{10}3_{10}3_{10}$ and $\beta\beta\beta$ motifs decreased with increasing length of peptide chain for the charged and blocked forms of poly-(Ala)_n and poly-(Gln)_n peptides consisting of the same number of amino acids.

In the case of α - and 3_{10} -helices as well as antiparallel β -strand, in addition to the conventional secondary structures occurring in the tripeptide units, helical and strand-like structures evolved in longer segments (i.e. tetra- and pentapeptide units, and so on) were also identified. These results showed that the number of longer periodic second-

Table 4 Relative populations (in %) compared to the total number of different tripeptide motifs (M_T) for the three conventional periodic secondary structures (α -helix: $\alpha\alpha\alpha$, 3_{10} -helix: $3_{10}3_{10}3_{10}$, β -strand:

$\beta\beta\beta$) and for the six non-conventional tripeptide motifs (HH β , H β H, β HH, H β β , β H β , β β H)

HOP	Motifs of tripeptide units									M_T
	$\alpha\alpha\alpha$	$3_{10}3_{10}3_{10}$	$\beta\beta\beta$	HH β	H β H	β HH	H $\beta\beta$	β H β	β β H	
H_3N^+ -(Ala) ₇ -COO [−]	13.2	17.5	8.4	3.3	12.0	14.4	10.2	13.8	7.2	794
H_3N^+ -(Ala) ₁₀ -COO [−]	17.0	22.2	7.7	3.6	9.9	12.4	9.2	9.9	8.1	1,378
H_3N^+ -(Ala) ₁₄ -COO [−]	20.4	26.5	5.8	3.4	7.9	13.1	7.3	7.8	7.8	2,317
H_3N^+ -(Ala) ₂₀ -COO [−]	19.9	26.2	8.7	3.0	8.4	11.7	7.3	7.5	7.3	3,602
$M_{\text{Ave}}^{\text{a}}$	17.6	23.1	7.7	3.3	9.6	12.9	8.5	9.8	7.6	
Ace-(Ala) ₇ -NMe	25.1	28.4	5.3	2.9	7.9	12.9	4.9	6.0	6.6	1,478
Ace-(Ala) ₁₀ -NMe	21.7	27.2	4.5	3.6	10.9	12.9	6.1	7.3	5.8	1,934
Ace-(Ala) ₁₄ -NMe	21.2	26.5	5.4	3.4	8.8	12.7	7.3	7.6	7.1	2,744
Ace-(Ala) ₂₀ -NMe	21.1	26.3	7.1	3.6	8.2	11.9	7.4	7.2	7.2	3,978
M_{Ave}	22.3	27.1	5.6	3.4	9.0	12.6	6.4	7.0	6.7	
H_3N^+ -(Gln) ₇ -COO [−]	4.9	12.0	15.2	6.2	10.0	9.4	16.8	15.5	10.0	309
H_3N^+ -(Gln) ₁₀ -COO [−]	5.1	15.2	17.6	5.8	7.9	10.5	13.4	13.2	11.3	591
H_3N^+ -(Gln) ₁₄ -COO [−]	7.8	17.5	14.0	4.8	7.7	9.1	12.8	13.5	12.8	1,027
H_3N^+ -(Gln) ₂₀ -COO [−]	7.2	15.8	14.1	6.0	8.3	8.9	14.1	14.2	11.4	1,509
M_{Ave}	6.3	15.1	15.2	5.7	8.5	9.5	14.3	14.1	11.4	
Ace-(Gln) ₇ -NMe	12.8	20.9	8.7	5.0	8.6	13.2	10.9	11.5	8.4	688
Ace-(Gln) ₁₀ -NMe	13.7	21.5	9.3	4.2	6.6	9.8	14.3	12.5	8.1	943
Ace-(Gln) ₁₄ -NMe	8.2	18.6	11.4	6.3	8.7	10.0	13.7	12.7	10.4	1,257
Ace-(Gln) ₂₀ -NMe	7.8	16.9	15.0	4.3	7.9	8.8	14.3	13.7	11.3	1,853
M_{Ave}	10.6	19.5	11.1	5.0	8.0	10.5	13.3	12.6	9.6	

^a $M_{\text{Ave}}-\text{s}$ are the average ratios of motifs (in %) for charged poly-(Ala)_n, blocked poly-(Ala)_n, charged poly-(Gln)_n and blocked poly-(Gln)_n peptides, respectively

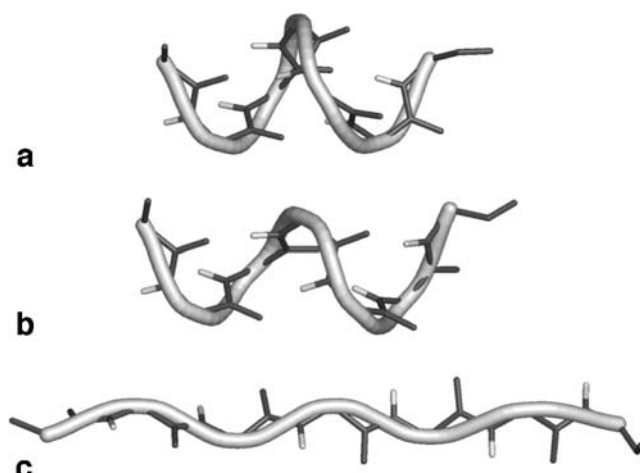


Fig. 2 Longest (a) α -helix, (b) 3_{10} -helix and (c) antiparallel β -strand observed in the $\text{H}_3\text{N}^+-(\text{Ala})_7-\text{COO}^-$ peptide. Only the peptide backbones are represented by both sticks and ribbon

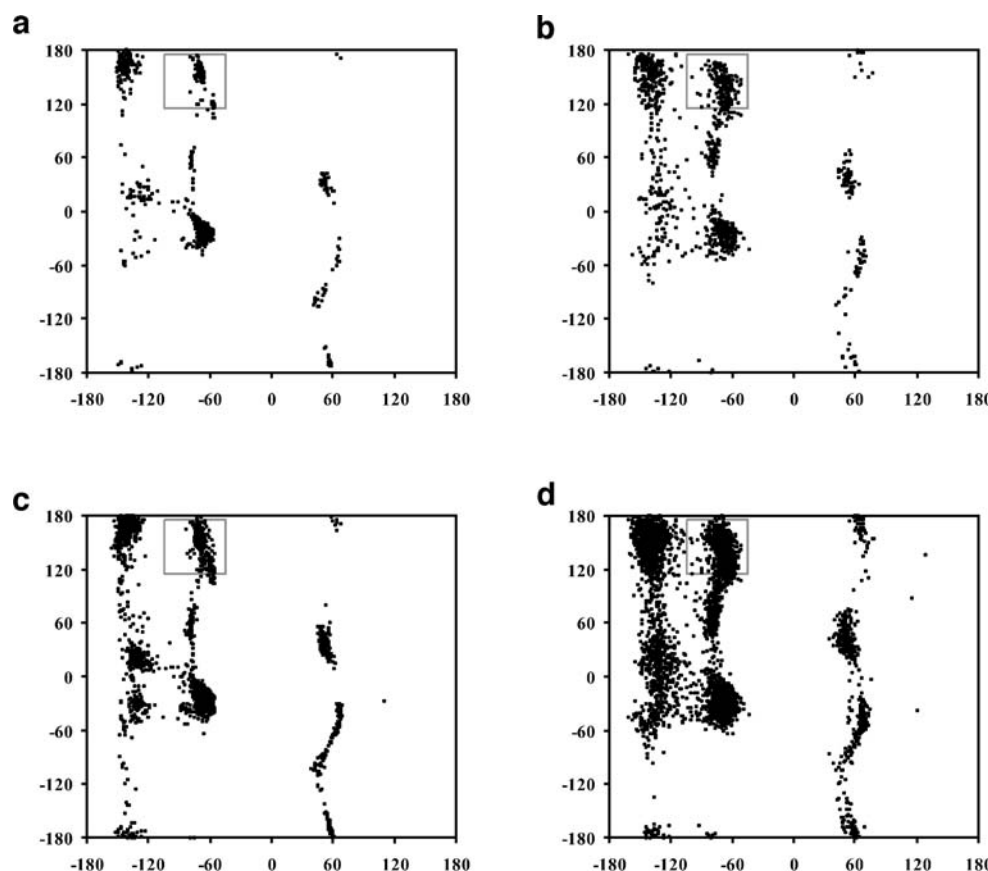
ary structures was smaller as compared to the populations observed in the tripeptide units. In the majority of cases, for peptides composed of 7 or 10 residues, conformers were found in which periodic secondary structures appeared along the whole length of HOPs, while for the peptides consisting of 14 or 20 amino acids, the longest helical or strand-like structures evolved in segments possessing a maximum of 10 amino acids. Figure 2 represents the

longest α -helix, 3_{10} -helix and antiparallel β -strand observed in the $\text{H}_3\text{N}^+-(\text{Ala})_7-\text{COO}^-$ peptide.

For the poly-(Ala)_n and poly-(Gln)_n peptides, small populations of the PPII helical segments were detected in tri- and tetrapeptide units. Recent experimental and theoretical studies performed on Ala- and Gln-based peptides as well as poly-(Gln) molecules have suggested the existence of local PPII conformation for individual Ala and Gln residues [22, 31–34]. Therefore, each Ala and Gln amino acid was examined for the presence of these local PPII structures along the entire sequence of poly-(Ala)_n and poly-(Gln)_n peptides. Our results showed that all individual Ala and Gln residues possessed a propensity to occupy the PPII helical conformation, and the populations of these local PPII structures were only slightly smaller compared to those found for the local α - and 3_{10} -helical, as well as local antiparallel β -strand, conformations. Figure 3 shows Ramachandran plots regarding individual Ala and Gln residues as well as all five Ala and Gln amino acids representing the local conformational states for the $\text{H}_3\text{N}^+-(\text{Ala})_7-\text{COO}^-$ and $\text{H}_3\text{N}^+-(\text{Gln})_7-\text{COO}^-$ peptides. In these Ramachandran plots, the characteristic PPII helical region is indicated and, as can be seen, a number of local conformations occupy the PPII structure for both Ala and Gln residues.

In addition to the conventional periodic secondary structures, other motifs occurring in the tripeptide units of

Fig. 3 Ramachandran plots of the individual (a) Ala⁴ and (b) Gln⁴ residues as well as the cumulated plots of all the five (c) Ala and (d) Gln amino acids for the $\text{H}_3\text{N}^+-(\text{Ala})_7-\text{COO}^-$ and $\text{H}_3\text{N}^+-(\text{Gln})_7-\text{COO}^-$ peptides. The characteristic PPII helical region is indicated by a grey square



these HOPs were examined. The presence of six different motifs ($\text{HH}\beta$, $\text{H}\beta\text{H}$, βHH , $\text{H}\beta\beta$, $\beta\text{H}\beta$ and $\beta\beta\text{H}$) was investigated, where the three letters relate to three consecutive amino acids. The α - and 3_{10} -helical regions were merged and labelled as H, because the characteristic ranges of Φ and Ψ torsion angles overlap for these two helices (see Table 1), while the antiparallel β -strand was labelled as β . Table 4 shows the relative populations of six non-conventional structural elements in the same way as it was done in the case of conventional secondary structures. Taking into account the values of M_{Ave} for these motifs, it can be seen that the populations of $\text{H}\beta\text{H}$ and βHH structures were larger, and the proportions of $\text{H}\beta\beta$, $\beta\text{H}\beta$ and $\beta\beta\text{H}$ motifs were lower for the poly-(Ala)_n peptides compared to those for the poly-(Gln)_n peptides, which can be explained by the greater propensity of poly-(Ala)_n molecules to form helical structures. If we consider the values of M_{T} , differences can be observed between the poly-(Ala)_n and poly-(Gln)_n peptides as well as between the charged and blocked forms of molecules. For the poly-(Ala)_n peptides, more tripeptide motifs appeared than for the poly-(Gln)_n peptides; furthermore, in the case of zwitterionic forms, the number of motifs was smaller compared to those for the terminally blocked forms.

Intramolecular H-bonds

For the conformers derived from SA calculations, intramolecular H-bonding patterns formed between the NH donor and CO acceptor groups were studied. In the case of both HOPs, H-bonds evolved by the participation of backbone

atoms were identified; however, for the poly-(Gln)_n peptides, H-bonds formed between the backbone and side-chain atoms as well as between the side-chain atoms of Gln amino acids were also examined.

Table 5 shows the minimum (H-bond_{min}), maximum (H-bond_{max}), average (H-bond_{ave}) populations and the total numbers (H-bond_{sum}) of $i \leftarrow i+3$ H-bonds between a backbone NH donor group of $i+3$ th and a CO acceptor group of i th residues for the poly-(Ala)_n and poly-(Gln)_n peptides. The $i \leftarrow i+3$ H-bonds appeared in each tetrapeptide segment along the entire sequence of molecules in accordance with the presence of type I and type III β -turns. The values of H-bond_{min}, H-bond_{max}, H-bond_{ave} and H-bond_{sum} indicated that larger proportions of the $i \leftarrow i+3$ H-bonds could be observed for the poly-(Ala)_n peptides compared to those for the poly-(Gln)_n peptides. This observation is in good agreement with the above-mentioned greater propensity of poly-(Ala)_n molecules to form different β -turns. In the case of charged peptides, the populations of $i \leftarrow i+3$ H-bonds were lower at the N- and C-terminal tetrapeptide segments in comparison with those observed at any other places. This correlated well with the smaller number of β -turns occurring in the two above-mentioned tetrapeptide units for the zwitterionic form of HOPs. All the minimum populations represented in Table 5 were located in either the N-terminal or the C-terminal tetrapeptide units for the charged HOPs.

The multiple turn structures described earlier showed characteristic H-bonding patterns in accordance with the occurrence of β -turns. In most cases, a β -turn structure evolved in any tetrapeptide unit was stabilised by an $i \leftarrow i+3$

Table 5 Minimum (H-bond_{min}), maximum (H-bond_{max}), average (H-bond_{ave}) populations (in number) and the total numbers (H-bond_{sum}) of $i \leftarrow i+3$ H-bonds formed between a backbone NH donor group of $i+3$ th and a CO acceptor group of i th residues

HOP	Populations of $i \leftarrow i+3$ H-bonds			
	H-bond _{min}	H-bond _{max}	H-bond _{ave}	H-bond _{sum}
$\text{H}_3\text{N}^+-(\text{Ala})_7-\text{COO}^-$	83	211	144	577
Ace-(Ala) ₇ -NMe	145	170	160	641
$\text{H}_3\text{N}^+-(\text{Gln})_7-\text{COO}^-$	33	88	67	268
Ace-(Gln) ₇ -NMe	90	112	102	409
$\text{H}_3\text{N}^+-(\text{Ala})_{10}-\text{COO}^-$	64	175	141	986
Ace-(Ala) ₁₀ -NMe	128	175	156	1,091
$\text{H}_3\text{N}^+-(\text{Gln})_{10}-\text{COO}^-$	30	89	65	453
Ace-(Gln) ₁₀ -NMe	72	94	86	602
$\text{H}_3\text{N}^+-(\text{Ala})_{14}-\text{COO}^-$	83	163	137	1,508
Ace-(Ala) ₁₄ -NMe	128	172	141	1,549
$\text{H}_3\text{N}^+-(\text{Gln})_{14}-\text{COO}^-$	32	81	64	699
Ace-(Gln) ₁₄ -NMe	61	93	72	791
$\text{H}_3\text{N}^+-(\text{Ala})_{20}-\text{COO}^-$	73	159	129	2,198
Ace-(Ala) ₂₀ -NMe	110	187	138	2,353
$\text{H}_3\text{N}^+-(\text{Gln})_{20}-\text{COO}^-$	23	77	55	941
Ace-(Gln) ₂₀ -NMe	49	80	64	1,087

H-bond; however, several β -turns that satisfied the Φ and Ψ torsion angle criteria, but lacked the stabilising H-bonds were also identified. Figure 4a shows the H-bonding pattern of a double turn structure found in the $\text{H}_3\text{N}^+(\text{Ala})_7\text{-COO}^-$ peptide that is represented in Fig. 1. In accordance with the presence of two type III β -turns in the N- and C-terminal tetrapeptide units, two $i \leftarrow i+3$ H-bonds can be observed, one of which is formed between the Ala^1 and Ala^4 residues, while the other is located between amino acids Ala^4 and Ala^7 .

The $i \leftarrow i+3$ H-bonds play an important role in the structural stabilisation not only of β -turns, but also of 3_{10} -helical segments. In the case of both HOPs, 3_{10} -helical structures appearing in longer segments were identified in which stabilising consecutive $i \leftarrow i+3$ H-bonds were observed. Figure 4b represents the characteristic H-bonding pattern for the longest 3_{10} -helix observed in the $\text{H}_3\text{N}^+(\text{Ala})_7\text{-COO}^-$ peptide shown in Fig. 2b. For this structure,

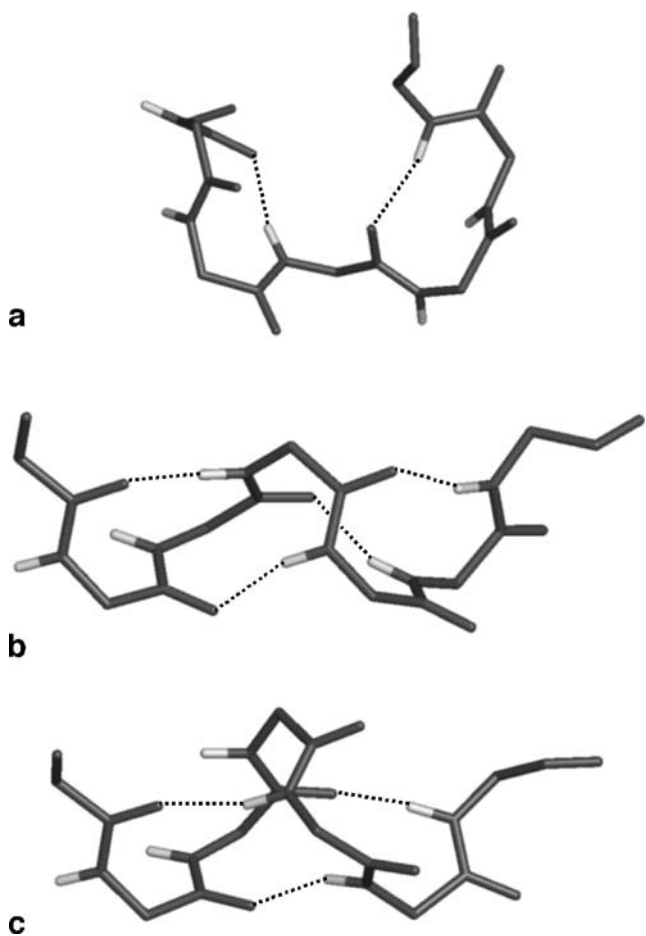


Fig. 4a–c H-bonding patterns of the conformers characterised by different secondary structural elements for the $\text{H}_3\text{N}^+(\text{Ala})_7\text{-COO}^-$ peptide. **a** A double turn structure with two H-bonds ($\text{Ala}^1 \leftarrow \text{Ala}^4$, $\text{Ala}^4 \leftarrow \text{Ala}^7$). **b** The longest 3_{10} -helix with four H-bonds ($\text{Ala}^1 \leftarrow \text{Ala}^4$, $\text{Ala}^2 \leftarrow \text{Ala}^5$, $\text{Ala}^3 \leftarrow \text{Ala}^6$, $\text{Ala}^4 \leftarrow \text{Ala}^7$). **c** The longest α -helix with three H-bonds ($\text{Ala}^1 \leftarrow \text{Ala}^5$, $\text{Ala}^2 \leftarrow \text{Ala}^6$, $\text{Ala}^3 \leftarrow \text{Ala}^7$). Only the peptide backbones are represented by sticks, and the dashed lines indicate the intramolecular H-bonds

four intramolecular $i \leftarrow i+3$ H-bonds can be found ($\text{Ala}^1 \leftarrow \text{Ala}^4$, $\text{Ala}^2 \leftarrow \text{Ala}^5$, $\text{Ala}^3 \leftarrow \text{Ala}^6$ and $\text{Ala}^4 \leftarrow \text{Ala}^7$), which prove the presence of the 3_{10} -helix evolved along the whole sequence of the peptide.

For poly-(Ala)_n and poly-(Gln)_n peptides, in addition to the presence of $i \leftarrow i+3$ H-bonds, the occurrence of $i \leftarrow i+4$ intramolecular H-bonds between the backbone atoms was also investigated, because they stabilise the α -helical structure. The distribution of $i \leftarrow i+4$ H-bonds was very similar to the distribution of α -helical segments observed for the HOPs. Comparing the populations of $i \leftarrow i+4$ H-bonds for either native poly-(Ala)_n and poly-(Gln)_n peptides or the charged and blocked forms of these molecules, similar observations could be made regarding the proportions of $i \leftarrow i+4$ H-bonds as for the relative populations of $\alpha\alpha\alpha$ motifs, as mentioned previously. Figure 4c shows the characteristic H-bonding pattern for the longest α -helix found in the $\text{H}_3\text{N}^+(\text{Ala})_7\text{-COO}^-$ peptide, which is represented in Fig. 2a. In this structure, three consecutive $i \leftarrow i+4$ H-bonds can be observed between the $\text{Ala}^1 \leftarrow \text{Ala}^5$, $\text{Ala}^2 \leftarrow \text{Ala}^6$ and $\text{Ala}^3 \leftarrow \text{Ala}^7$ amino acid pairs, which correspond to the α -helix appearing along the entire sequence of the peptide.

In the case of blocked peptides, several H-bonds formed by the participation of the Ace group as acceptor and the NMe group as donor that could take part in the further structural stabilisation of the N- and C-terminal ends of molecules were identified. For the charged forms of both HOPs, the NH group of the first three amino acids at the N-terminal end, and the CO group of the last three residues at the C-terminal end showed a lower propensity to participate in H-bonds, while for the blocked forms, only the NH group of first two and the CO group of last two amino acids showed similar properties. The reason for this is the effect of the Ace and NMe blocking groups, which can take part in the formation of further H-bonds as acceptors and donors, respectively. The lower propensity of the NH and the CO groups to form H-bonds at both the N- and the C-terminal ends of the peptides can be connected with the $i \leftarrow i+3$ H-bonds, since the first two or three N-terminal NH groups and the last two or three C-terminal CO groups, depending on the ionisation state, cannot form such H-bonds because of the lack of possible acceptor and donor partners, respectively. In the case of poly-(Ala)_n peptides, the NH and CO groups of the fourth amino acids for the charged forms and the same groups of the third residues for the blocked forms (counting from both the N- and the C-terminal ends), showed somewhat similar features, which are related to the $i \leftarrow i+4$ H-bonds and the lack of possible acceptor and donor partners, like in the case of $i \leftarrow i+3$ H-bonds. For poly-(Gln)_n peptides, these properties were not observed, probably due to the lower propensity of these HOPs to form α -helical structures.

Beside the H-bonds evolving between the backbone atoms, in the case of poly-(Gln)_n peptides, further intramolecular H-bonds appearing via the participation of NH and CO groups of Gln side-chains were also examined. Three different types of such H-bonds could be distinguished considering that they could involve the NH donor and CO acceptor groups of both backbone and side-chain of the Gln amino acids: (1) H-bonds between the backbone NH and side-chain CO groups (NH_B-CO_S, where the B and S letters in subscript denote backbone and side-chain, respectively), (2) H-bonds between the side-chain NH and backbone CO groups (NH_S-CO_B), and (3) H-bonds between the side-chain NH and side-chain CO groups (NH_S-CO_S). The intramolecular H-bonds mentioned above might have an effect on the populations of evolving secondary structural elements (β -turns, α - and 3_{10} -helices), because they can decrease the proportions of H-bonds formed between the backbone atoms that stabilise the turn and helical structures. For poly-(Gln)_n peptides, the smaller populations of secondary structural elements, described earlier, can be explained by the formation of NH_B-CO_S, NH_S-CO_B and NH_S-CO_S H-bonds. Comparing the ratios of these H-bonds relative to one another, the NH_S-CO_B H-bonds appeared in the largest number, while the proportion of NH_B-CO_S H-bonds was the lowest. Nevertheless, the majority of NH_B-CO_S, NH_S-CO_B and NH_S-CO_S H-bonds were formed between any *i*th residue and its three preceding or following neighbours ($i-3 \leftarrow i$, $i-2 \leftarrow i$, $i-1 \leftarrow i$ H-bonds and $i \rightarrow i+1$, $i \rightarrow i+2$, $i \rightarrow i+3$ H-bonds).

Conclusions

We performed a conformational analysis of both charged and terminally blocked forms of poly-(Ala)_n and poly-(Gln)_n peptides of different lengths. For the conformers obtained by SA calculations, detailed structural investigation concerning the secondary structural elements and the intramolecular H-bonding patterns was carried out. The results of our conformational study indicated that, for both the poly-(Ala)_n and the poly-(Gln)_n peptides, various secondary structural elements (type I and type III β -turns, α -helix, 3_{10} -helix, antiparallel β -strand) could be observed. In the case of both HOPs, β -turns appeared in every tetrapeptide segment along the entire sequence of the peptides, while periodic secondary structural elements evolved mainly in tri- and tetrapeptide units; however, longer helices and strands could also be found in smaller numbers. In accordance with the occurrence of turns and helical structures, characteristic H-bonding patterns formed either by $i \leftarrow i+3$ or by $i \leftarrow i+4$ H-bonds were identified. Considering the populations of secondary structural elements and intramolecular H-bonds, differences could be

found either between the poly-(Ala)_n and poly-(Gln)_n peptides or between the charged and blocked forms of these molecules. Poly-(Ala)_n peptides showed a greater propensity to form β -turns and helical structures compared to poly-(Gln)_n peptides; however, for the populations of antiparallel β -strand, the relationship was the opposite between the two HOPs. Nevertheless, in the majority of cases, the terminally blocked peptides contained more secondary structural elements as compared to the zwitterionic molecules. Taking into account intramolecular H-bonds, similar differences could be found between the two forms of HOPs depending on their ionisation state, as for the secondary structures.

Our results showed that poly-(Ala)_n peptides contained mainly α - and 3_{10} -helical segments as periodic secondary structural elements. This corresponds to the high propensity of alanine to form helical structures and to the results of earlier investigations suggesting either α -helix [4–9] or 3_{10} -helix [10–12] as the characteristic conformation. Contrary to earlier experimental [13, 14] and theoretical [15, 16] investigations, in which PPII conformation was detected for both poly-(Ala) and Ala-based peptides, we did not find a significant amount of this helical structure evolved in three or more consecutive residues. However, a considerable number of local PPII conformations was observed for all individual Ala residues, similarly to the case of the Ala-based peptide, XAO [31–33]. Beside the helical structures, we identified either single or multiple β -turns for the poly-(Ala)_n peptides, which appeared along the entire sequence of the molecules. Our findings correspond to recent observations concerning the structural properties of XAO peptide [31, 33]. Nevertheless, as it was pointed out previously, the above-mentioned turn structures play an important role in the initiation of helix formation, and they appear as intermediate states during the random-coil-to-helix transition and in the folding process [9, 35–37].

In the case of poly-(Gln)_n molecules, mostly 3_{10} -helical and antiparallel β -strand-like segments were observed as periodic structures. The presence of the latter secondary structural element is in agreement with the previous observation that a peptide composed of 15 Gln residues adopts a β -structure made of antiparallel β -strands [23]. Nevertheless, we also observed β -turns, which might play a role in the formation of hairpin conformations, as observed previously [23, 24]. As with poly-(Ala)_n peptides, local conformational states characterised by PPII structure were found in the case of all individual Gln residues, as it was recently proposed for poly-(Gln) and Gln-based molecules [22, 34]. Earlier experimental and theoretical studies also suggested a random coil or unordered conformation for poly-(Gln) and Gln-based peptides [20–22]. Beside the β -turns, 3_{10} -helical and antiparallel β -strand-like segments, our conformational analysis also revealed random coil structures.

Finally, from the results of our conformational analysis of poly-(Ala)_n and poly-(Gln)_n peptides, it can be concluded that both HOPs exist as an ensemble of conformational states characterised by a variety of secondary structural elements. Nevertheless, our detailed structural investigation yielded several results that will be useful in our forthcoming studies, and which will help provide deeper insights into the mechanism of the formation of human illnesses and neurodegenerative diseases involving HOPs.

Acknowledgements This research was supported by grants GVOP-3.1.1.-2004-05-0492/3.0 and RET 08/2004.

References

- Brown LY, Brown SA (2004) Trends Genet 20:51–58
- Perutz MF (1996) Curr Opin Struct Biol 6:848–858
- Perutz MF (1999) Trends Biochem Sci 24:58–63
- Ripoll DR, Scheraga HA (1988) Biopolymers 27:1283–1303
- Mortenson PN, Wales DJ (2001) J Chem Phys 114:6443–6454
- Mortenson PN, Evans DA, Wales DJ (2002) J Chem Phys 117:1363–1376
- Daggett V, Kollman PA, Kuntz ID (1991) Biopolymers 31:1115–1134
- Bertsch RA, Vaidehi N, Chan SI, Goddard III WA (1998) Proteins 33:343–357
- Takano M, Yamato T, Higo J, Suyama A, Nagayama K (1999) J Am Chem Soc 121:605–612
- Fiori WR, Miick SM, Millhauser GL (1993) Biochemistry 32:11957–11962
- Miick SM, Martinez GV, Fiori WR, Todd AP, Millhauser GL (1992) Nature 359:653–655
- Miick SM, Casteel KM, Millhauser GL (1993) Biochemistry 32:8014–8021
- Shi Z, Olson CA, Rose GD, Baldwin RL, Kallenbach NR (2002) Proc Natl Acad Sci USA 99:9190–9195
- McColl IH, Blanch EW, Hecht L, Kallenbach NR, Barron LD (2004) J Am Chem Soc 126:5076–5077
- Kentsis A, Mezei M, Gindin T, Osman R (2004) Proteins 55:493–501
- Mezei M, Fleming PJ, Srinivasan R, Rose GD (2004) Proteins 55:502–507
- Garcia AE (2004) Polymer 45:669–676
- Levy Y, Jortner J, Becker OM (2001) Proc Natl Acad Sci USA 98:2188–2193
- Ross CA, Poirier MA, Wanker EE, Amzel M (2003) Proc Natl Acad Sci USA 100:1–3
- Altschuler EL, Hud NV, Mazrimas JA, Rupps B (1997) J Pept Res 50:73–75
- Chen S, Berthelier V, Yang W, Wetzel R (2001) J Mol Biol 311:173–182
- Wang X, Vitalis A, Wyczalkowski MA, Pappu RW (2006) Proteins 63:297–311
- Perutz MF, Johnson T, Suzuki M, Finch JT (1994) Proc Natl Acad Sci USA 91:5355–5358
- Sharma D, Sharma S, Pasha S, Brahmachari SK (1999) FEBS Lett 456:181–185
- Perutz MF, Finch JT, Berriman J, Lesk A (2002) Proc Natl Acad Sci USA 99:5591–5595
- Stork M, Giese A, Kretzschmar HA, Tavan P (2005) Biophys J 88:2442–2451
- Case DA, Darden TA, Cheatham III TE, Simmerling CL, Wang J, Duke RE, Luo R, Merz KM, Pearlman DA, Crowley M, Walker RC, Zhang W, Wang B, Hayik S, Roitberg A, Seabra G, Wong KF, Paesani F, Wu X, Brozell S, Tsui V, Gohlke H, Yang L, Tan C, Mongan J, Hornak V, Cui G, Beroza P, Mathews DH, Schafmeister C, Ross WS, Kollman PA (2006) AMBER 9, University of California, San Francisco
- Wang J, Cieplak P, Kollman PA (2000) J Comput Chem 21:1049–1074
- Hawkins GD, Cramer CJ, Truhlar DG (1996) J Phys Chem 100:19824–19839
- Hawkins GD, Cramer CJ, Truhlar DG (1995) Chem Phys Lett 246:122–129
- Makowska J, Rodziewicz-Motowidlo S, Baginska K, Vila JA, Liwo A, Chmurzynski L, Scheraga HA (2006) Proc Natl Acad Sci USA 103:1744–1749
- Makowska J, Rodziewicz-Motowidlo S, Baginska K, Makowski M, Vila JA, Liwo A, Chmurzynski L, Scheraga HA (2007) Biophys J 92:2904–2917
- Schweitzer-Stennet R, Measey TJ (2007) Proc Natl Acad Sci USA 104:6649–6654
- Chellgren BW, Miller A-F, Creamer TP (2006) J Mol Biol 361:362–371
- Daggett V, Levitt M (1992) J Mol Biol 223:1121–1138
- Huo S, Straub JE (1999) Proteins 36:249–261
- Ding F, Borreguero JM, Buldyrey SV, Stanley HE, Dokholyan NV (2003) Proteins 53:220–228